



Progress of simulation study for heat handling and impurity seeding in the DEMO divertor

N. Asakura, K. Shimizu, K. Tobita
Japan Atomic Energy Agency, Naka

**US-Japan Workshop on Fusion Power Plants
and Related Advanced Technologies
NIFS, 22-24 Feb. 2011**

CONTENTS

1. Introduction: **Power handling in DEMO divertor**
2. Power exhaust simulation from SOLDOR&NEUT2D to “SONIC”
3. Development of SONIC for application to the DEMO divertor
4. Extension of ITER divertor concept to DEMO divertor ?
5. Summary

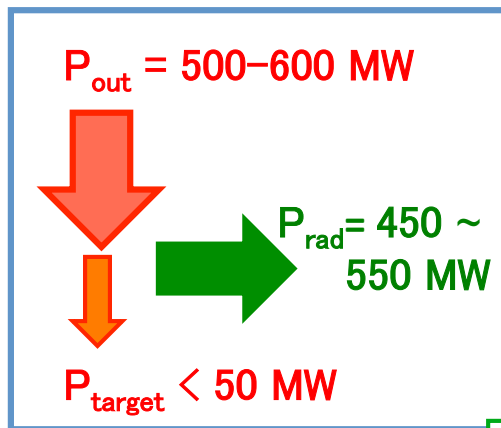
1. Introduction: power handling in DEMO reactor

- Power handling by plasma operation, divertor design and target engineering is the most important issue for the reactor design.

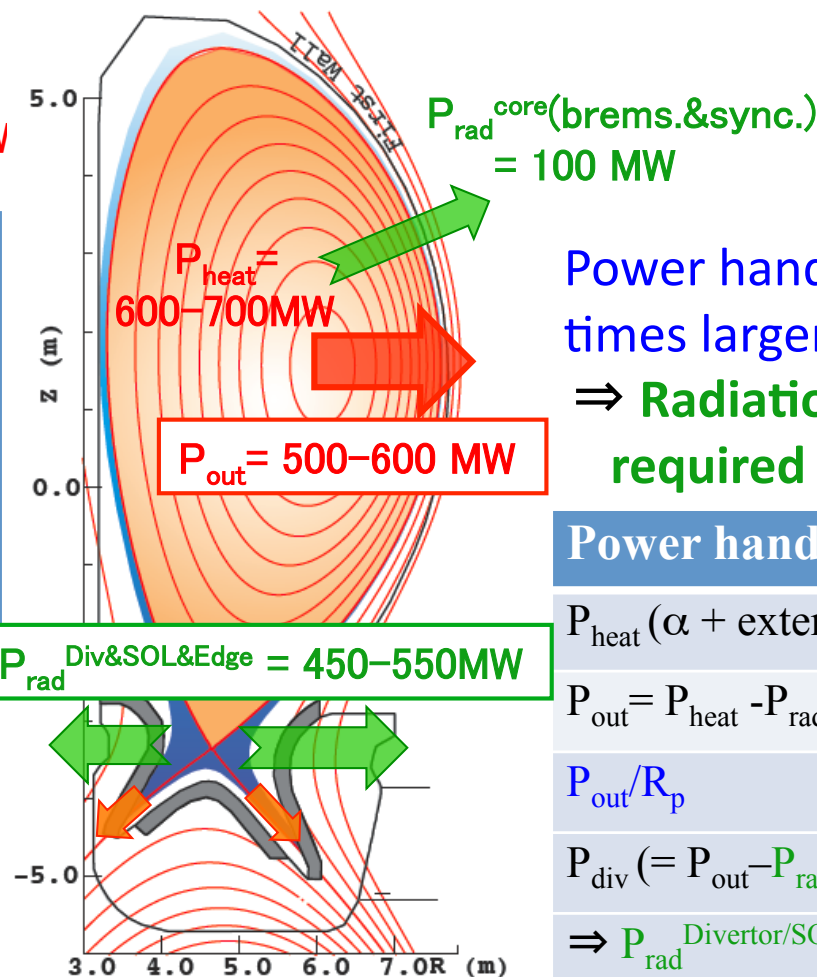
“*SlimCS*” aims $P_{fus} \leq 3$ GW ($P_{heat} = 600\sim 700$ MW) with reduced-size CS ($R = 5.5$ m and $A=2.6$) \Rightarrow Power exhausting to SOL is 5-6 times larger and R is smaller than ITER.

SlimCS

$P_{fusion} = 2.95$ GW
 $(P_{heat} = P_{\alpha} + P_{ax} = 600\sim 700$ MW)



Major radius : $R_p = 5.5$ m
 Minor radius : $a_p = 2.1$ m
 Plasma current : $I_p = 16.7$ MA
 Toroidal field : $B_t = 6.0$ T
 Plasma volume: $V_p = 941$ m³



Power handling factor (P/R) is 6-7 times larger than ITER
 \Rightarrow Radiation loss in edge/divertor is required 10 times larger than ITER

Power handle	SlimCS	ITER
$P_{heat} (\alpha + external)$	650 MW	150 MW
$P_{out} = P_{heat} - P_{rad}^{core}$	550 MW	100 MW
P_{out}/R_p	100MW/m	16MW/m
$P_{div} (= P_{out} - P_{rad}^{D/S/E})$	<50MW	~50MW
$\Rightarrow P_{rad}^{Divertor/SOL/Edge}$	~500MW	~50MW

Extension of ITER divertor concept to DEMO divertor ?

Design concept for ITER divertor is applied/extended to the DEMO (SlimCS) divertor: “divertor detachment” ($T_e \sim$ a few eV) is a key for the power handling

(1) Divertor leg and inclination of the target are larger than ITER

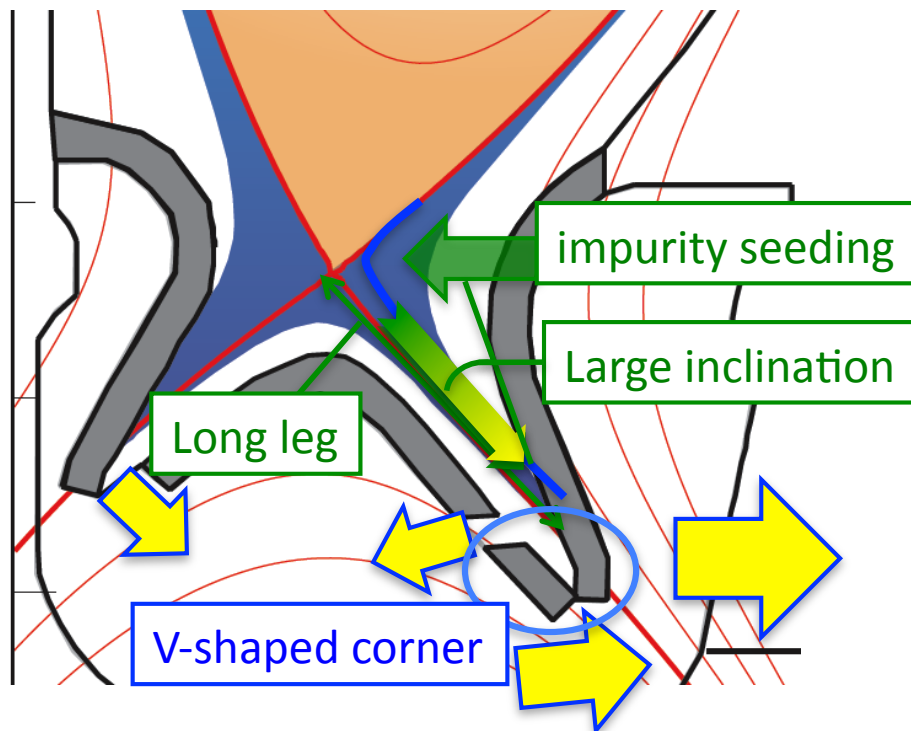
⇒ increase radiation, CX & volume recombination at the upstream, reducing q^{target} .

(2) V-shaped corner ⇒ enhance recycling near the strike-point.

(3) Impurity seeding such as Ne, N₂, Ar, Kr, Xe ⇒ enhance edge & divertor radiation.

⇔ Flux expansion is smaller than ITER due to longer distance of Div-coil from plasma

⇒ Effective wet area is comparable to ITER



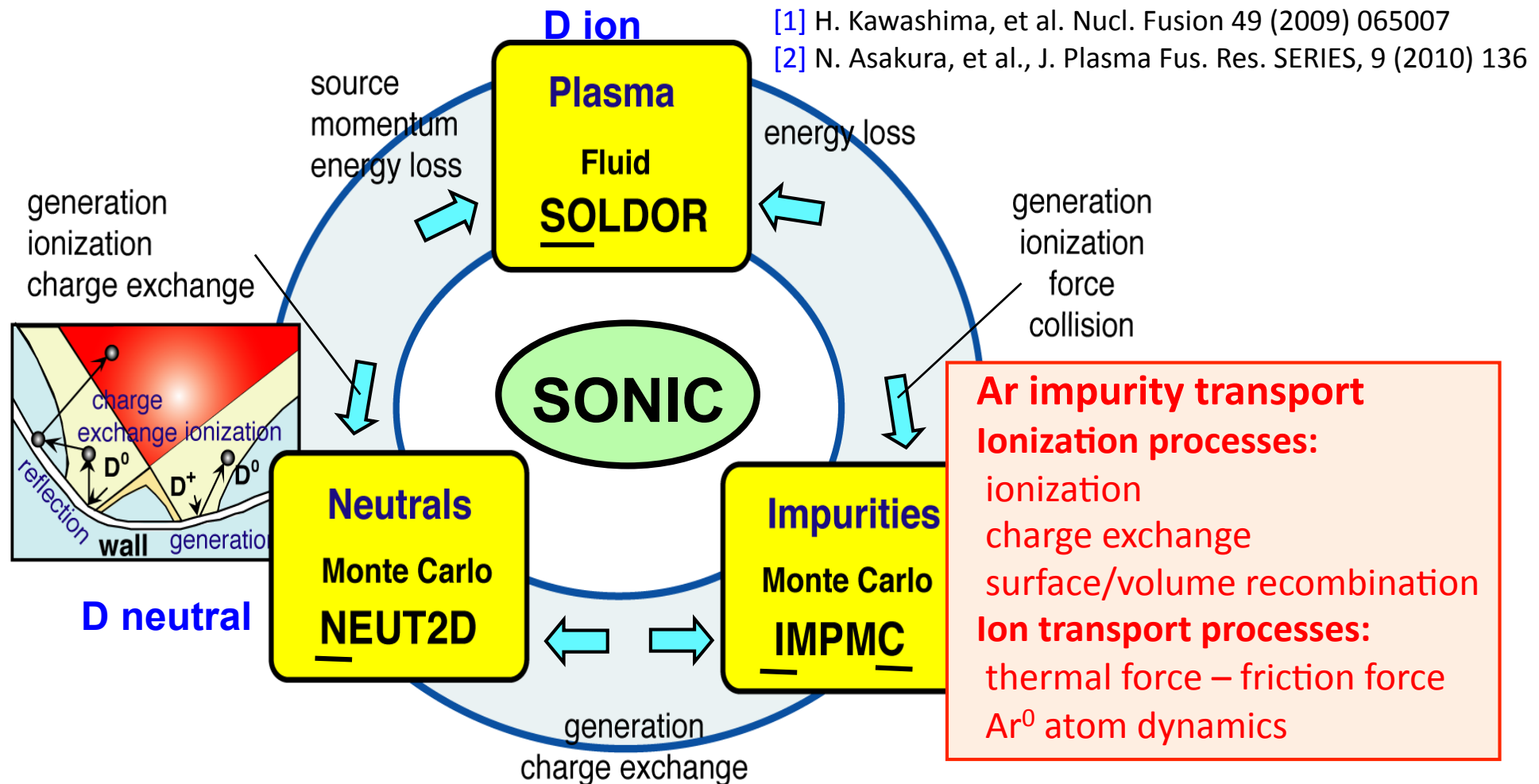
geometry parameters	SlimCS (2008)	ITER
leg length, L_{sp} (in/out)	1.37/1.83m	0.97/1.14m
incl. angle, θ_{sp} (in/out)	21°/18°	38°/25°
Dome top below Xp	~0.5m	~0.55m*
V-shaped corner	out **	in & out
Flux expansion(in)/(out)	7/3	7/6
Wet area for $\lambda_q^{\text{mid}} = 5\text{mm}$ (in/out)	2.2/1.9m ²	1.4/1.9m ²

* Lower dome design (2009)

** Inner divertor is detached without V-corner

2. Power exhaust simulation from SOLDOR&NEUT2D to “SONIC”: self-consistent coupling with impurity Monte Carlo has been developed

- **SOLDOR/NEUT2D** were used for DEMO divertor design, where Ar impurity radiation with *non-coronal model*: $P_{rad} = L(T_e, \tau_r) n_z n_e$, and constant n_{Ar}/n_i was applied. [1]
- **SONIC** was applied for SlimCS divertor simulation with Ar seeding. [2]



Power handling in DEMO divertor: full detachment is necessary

SOLDOR/NEUT2D results: full detachment in the outer divertor was obtained with increasing to $n_{Ar}/n_i = 5\%$ (outer divertor), where $n_{Ar}/n_i = 1\%$ (SOL & inner divertor).

Input parameters at edge-SOL

$$P_{out} = 500 \text{ MW}, \Gamma_{out} = 0.5 \times 10^{23} \text{ s}^{-1} (r/a=0.95)$$

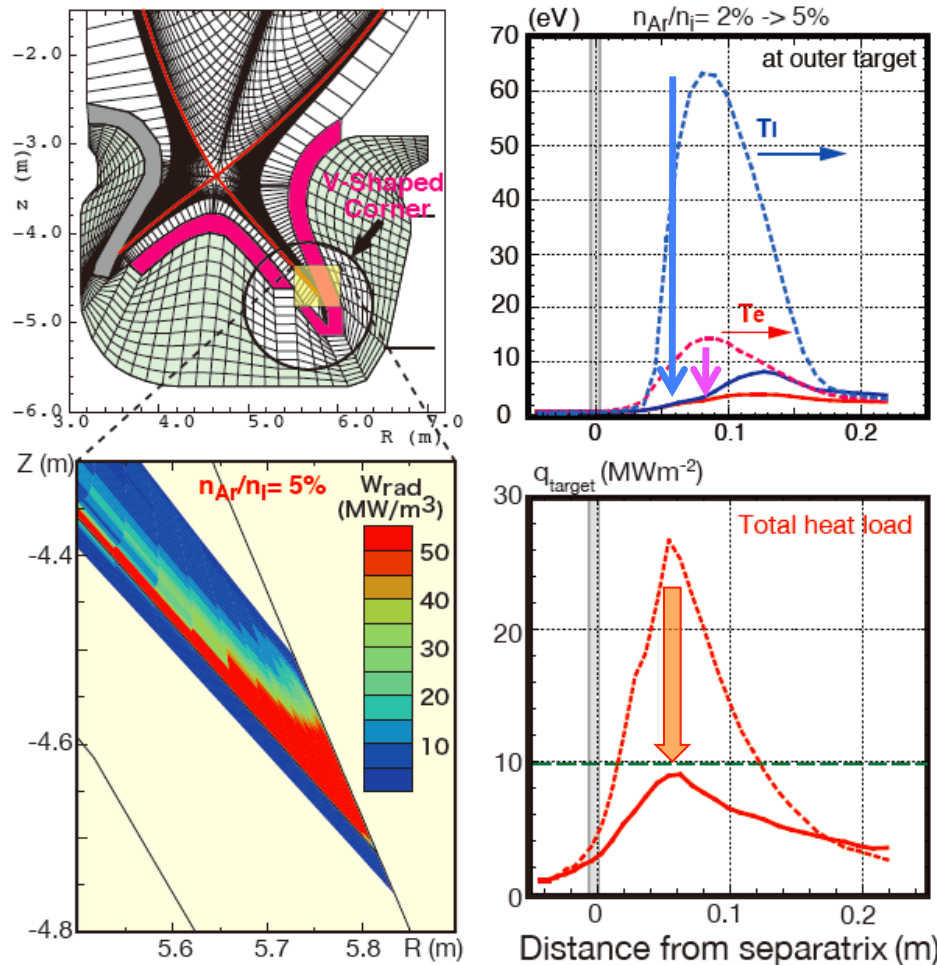
$$\chi_i = \chi_e = 1 \text{ m}^2 \text{ s}^{-1}, D = 0.3 \text{ m}^2 \text{ s}^{-1}$$

H. Kawashima, et al. Nucl. Fusion 49 (2009) 065007

D_2/T_2 gas puff: $\Gamma_{puff} = 1 \times 10^{23} \text{ s}^{-1}$ (200 $\text{Pam}^3 \text{ s}^{-1}$),

Divertor pumping speed at exhaust duct:

$S_{pump} = 200 \text{ m}^3 \text{ s}^{-1}$ is given.



- At the inner target, divertor is detached, and $q_{target} < 5 \text{ MW/m}^2$.
- Outer q_{target} decreases from 26 to 9 MWm^{-2} with increasing $n_{Ar}/n_i = 2\%$ to 5%
 \Rightarrow Full divertor detachment ($T_e \sim T_i < 3 \text{ eV}$) is obtained near strike-point ($\Delta d < 8 \text{ cm}$).
- Heat load extends in a wide divertor area, when P_{rad}^{tot}/P_{out} increased to $\sim 98\%$
 \Rightarrow Full detachment is necessary, but impurity transport was not included.

Power loadings by Radiation and Recombination become dominant ⇒ Impurity transport and neutral process become important

- Evaluation of major heat load on the target

$$q_{\text{target}} = \underbrace{\gamma \cdot n_d \cdot C_{sd} \cdot T_d}_{\text{Transport component}} + \underbrace{n_d \cdot C_{sd} \cdot E_{\text{ion}}}_{\text{Surface-recombination loss}} + \underbrace{f_1(P_{\text{rad}})}_{\text{Radiation power load}} + \underbrace{f_2(1/2 m v_0^2 n_0 v_0)}_{\text{Neutral power load}}$$

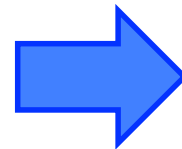
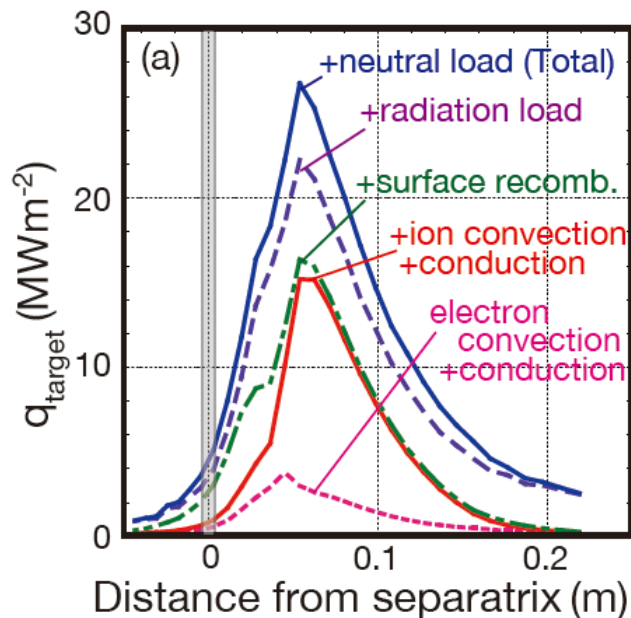
Transport component
 (incl. electron&ion-
 conduction/convection)

Surface-recombination
 loss

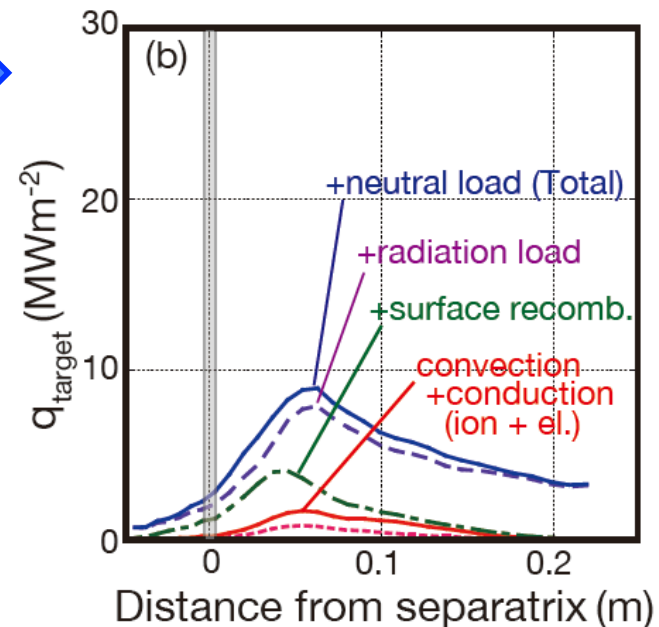
Radiation
 power load

Neutral
 power load

“V-shaped divertor” ($n_{\text{Ai}}/n_i=2\%$)



“V-shaped divertor” ($n_{\text{Ai}}/n_i=5\%$)



3. Development of SONIC for application to the DEMO divertor

Previous results was up to time scale of impurity (Ar) transport in the divertor ($t = 50$ ms), and Ar ions and radiation region were localized near target plate more than SOLDOR/NEUT2D results.

- **Recent development in SONIC simulation for demo divertor design:** conversion of divertor plasma parameters became more stable by introducing
 - (1) **“flux limiter” for ion conduction transport** : $q_i^{\text{conv}} = n_i k(T_i^{5/2}) \nabla T_i < 0.5 n_i v_{\text{th}-i} T_i$,
 - (2) **distribution of Ar atoms and particle balance under the divertor (exhaust route)**, which were calculated in the similar condition (simulating a steady-state), and some minor corrections such as $D_{\text{imp}} = 0.3 \Rightarrow 0.6 \text{ m}^2/\text{s}$, etc.

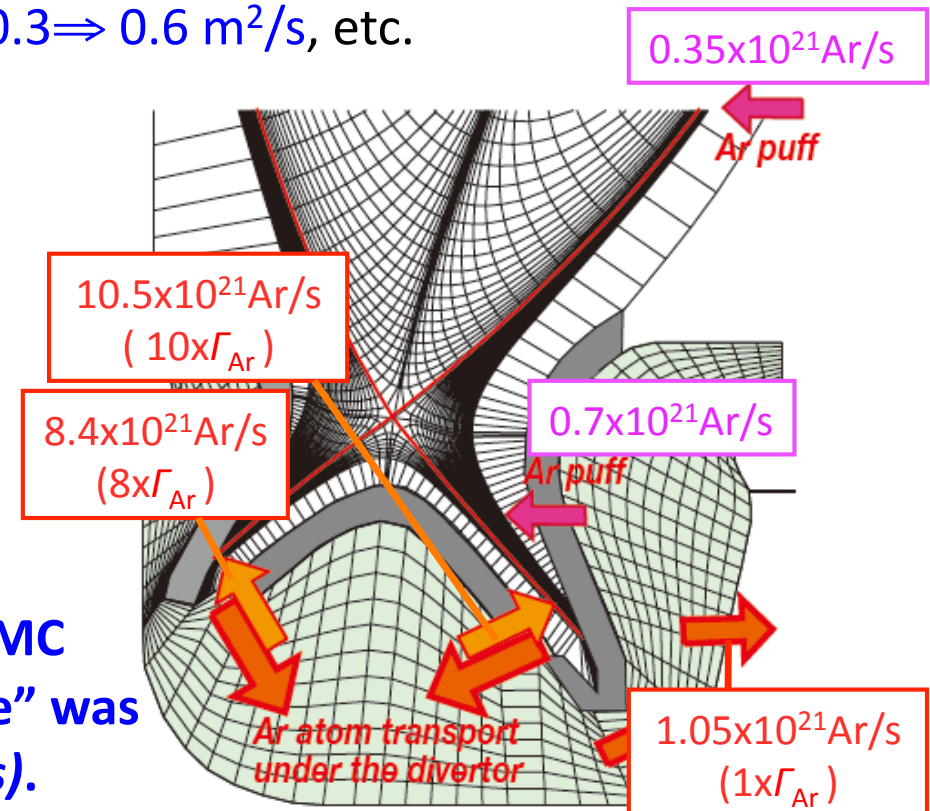
Ar puff location (outer midplane) was added as well as that at the outer divertor:

ex. For the case of the detached divertor:

$\Rightarrow \Gamma_{\text{Ar}}^{\text{div}} = 0.7 \times 10^{21} \text{ Ar/s}$ ($1.4 \text{ Pam}^3\text{s}^{-1}$) and $\Gamma_{\text{Ar}}^{\text{mid}} = 0.35 \times 10^{21} \text{ Ar/s}$ ($0.7 \text{ Pam}^3\text{s}^{-1}$), and

Ar backflow from exhaust slots (2) was handled as gas puff: $\Gamma_{\text{Ar}}^{\text{dom}}(\text{in}) = 8.4 \times 10^{21} \text{ Ar/s}$ ($17 \text{ Pam}^3\text{s}^{-1}$) and $\Gamma_{\text{Ar}}^{\text{dom}}(\text{out}) = 10.5 \times 10^{21} \text{ Ar/s}$ ($21 \text{ Pam}^3\text{s}^{-1}$).

Self-consistent coupling of the fluid plasma, MC neutral and MC impurity (Ar) “in steady-state” was obtained *with comparable time scale (~50ms)*.

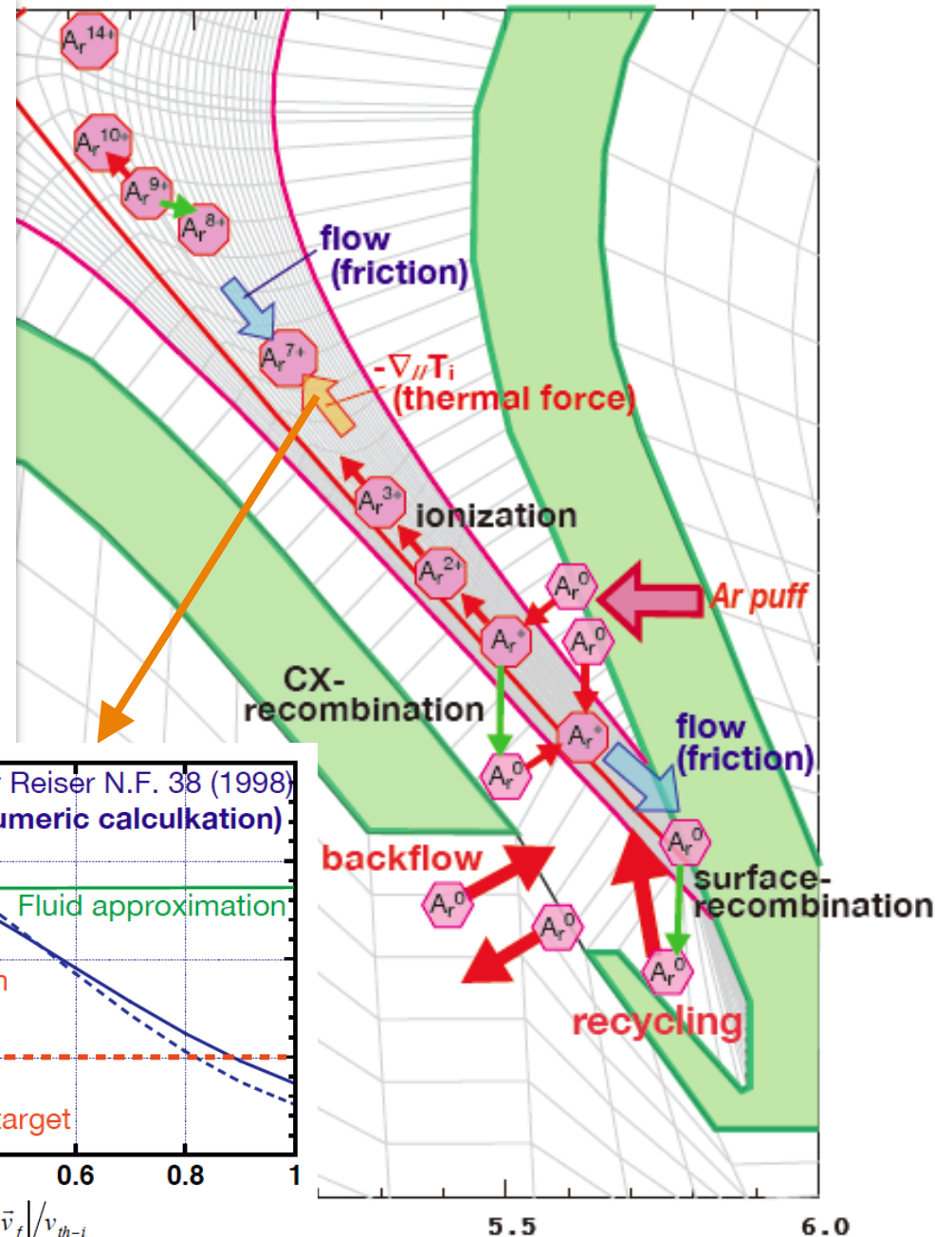
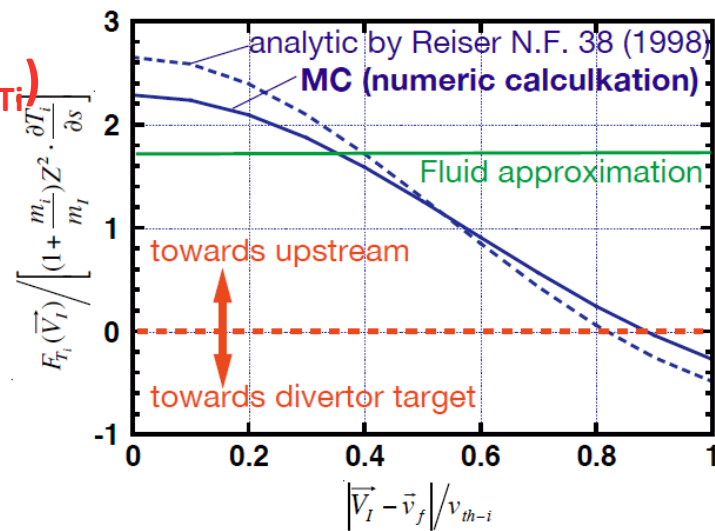


MC approach has advantages to impurity modelling

Most impurity transport processes are incorporated in original formula:

- Tracking impurity neutrals and ions
 \Rightarrow CX-loss, n-collision, recycling etc.
Radiation & Recombination at multi-charge states
- **Kinetic effect** \Rightarrow **Thermal force**
- **Gyro-motion** \Rightarrow **Erosion (for PWI)**

Kinetic thermal force (F_{Ti})
 decreases with
 impurity ion speed (v_i)
 approaching to ion
 thermal velocity (v_{th-i}).

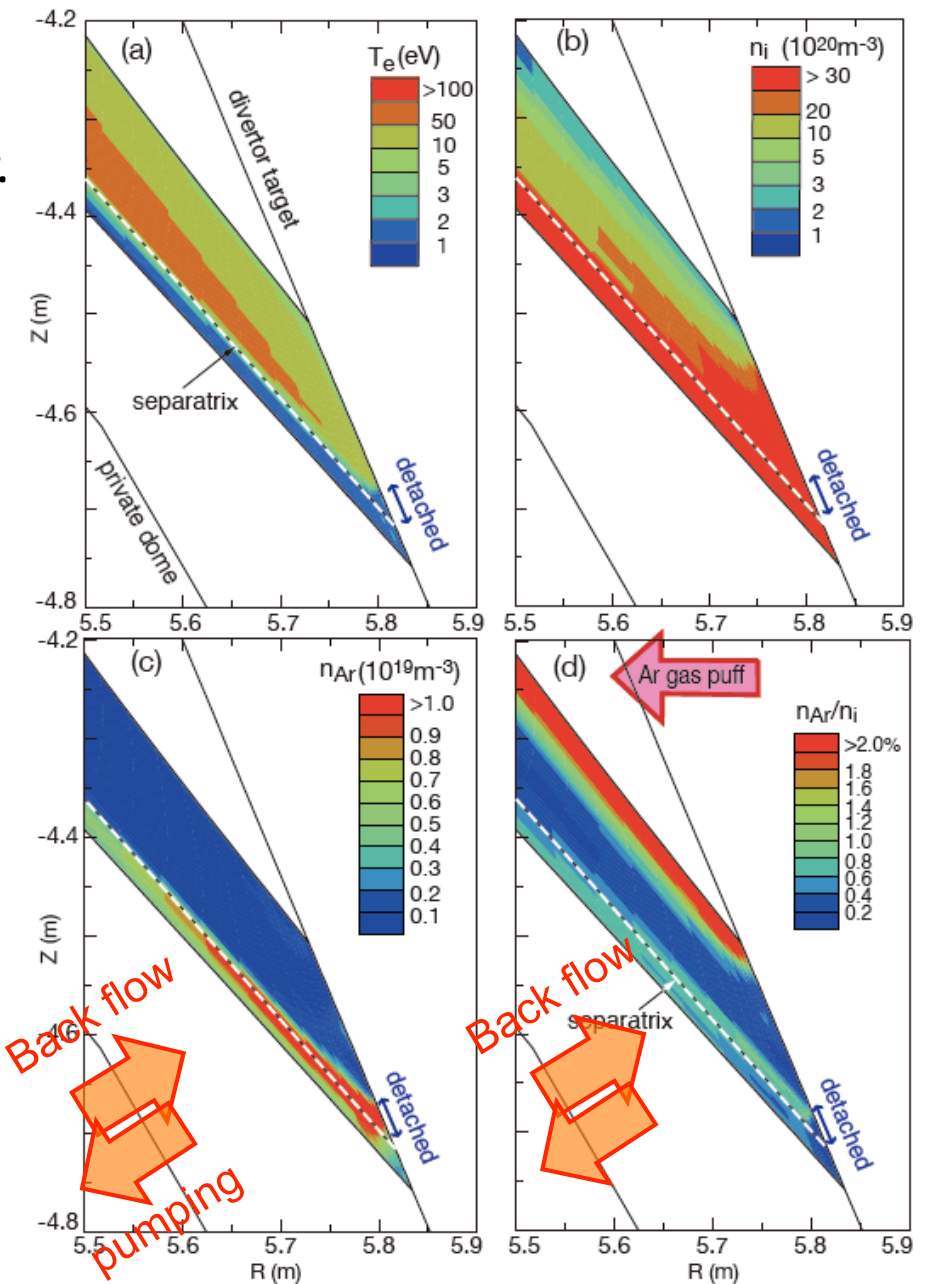
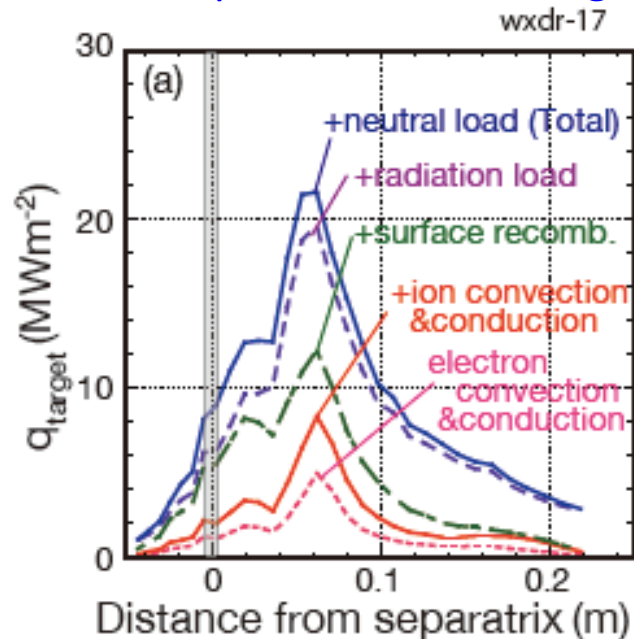


Detachment was produced by SONIC simulation with $P_{\text{rad}}^{\text{tot}} = 425\text{MW}$

Detachment near outer strike-point (*Low T_e & $T_i < 2\text{ eV}$ in $< 4\text{cm}$*) appears with increasing Ar puff rate both from midplane and divertor.

High $n_{\text{Ar}}/n_i \sim 4\%$ was seen at the outer flux surfaces (d) due to gas puff from outboard and large friction force, while it was low ($\sim 0.5\%$) near separatrix (c) under large Ar backflow and recycling flux.

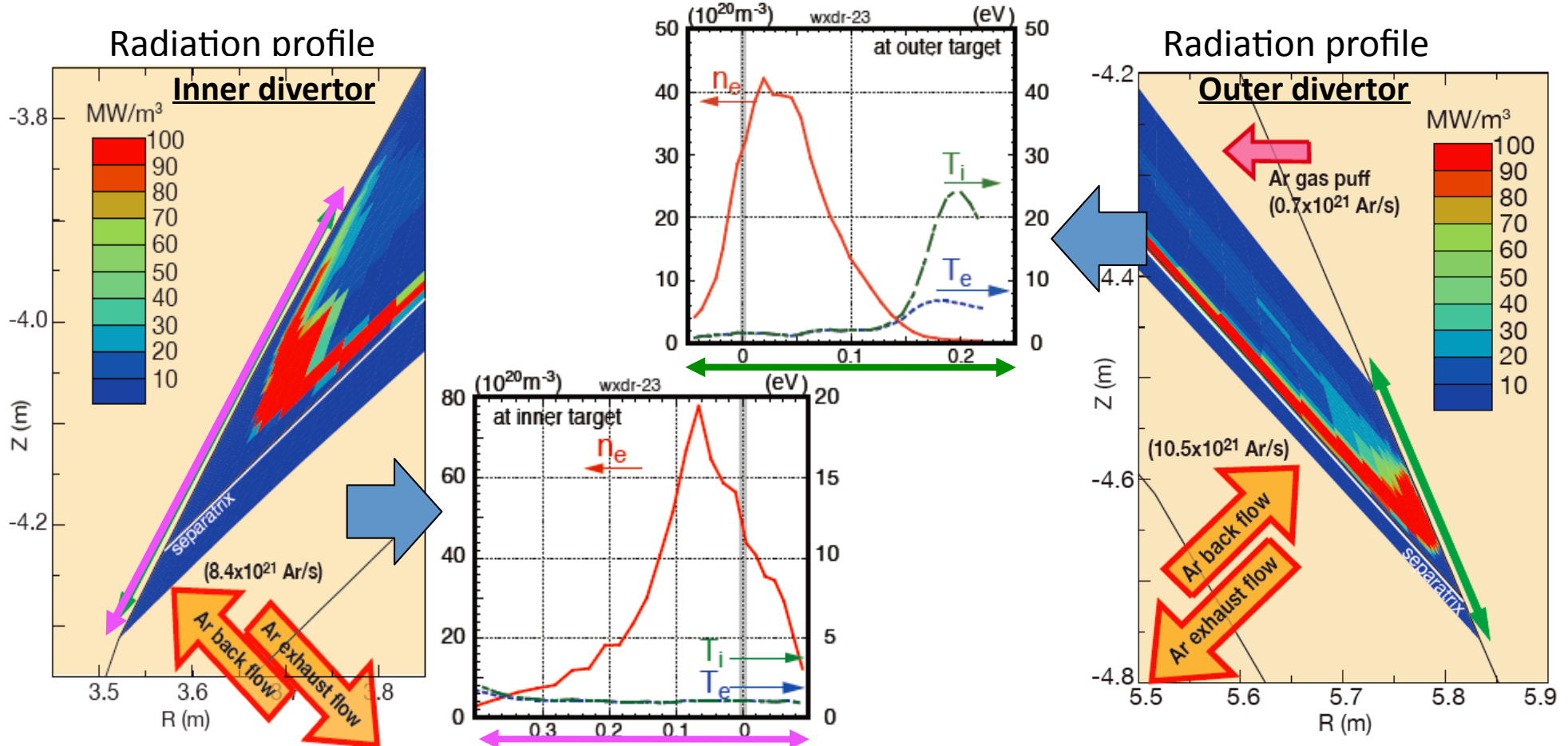
Heat load profile at outer target



Full detachment was produced by SONIC simulation

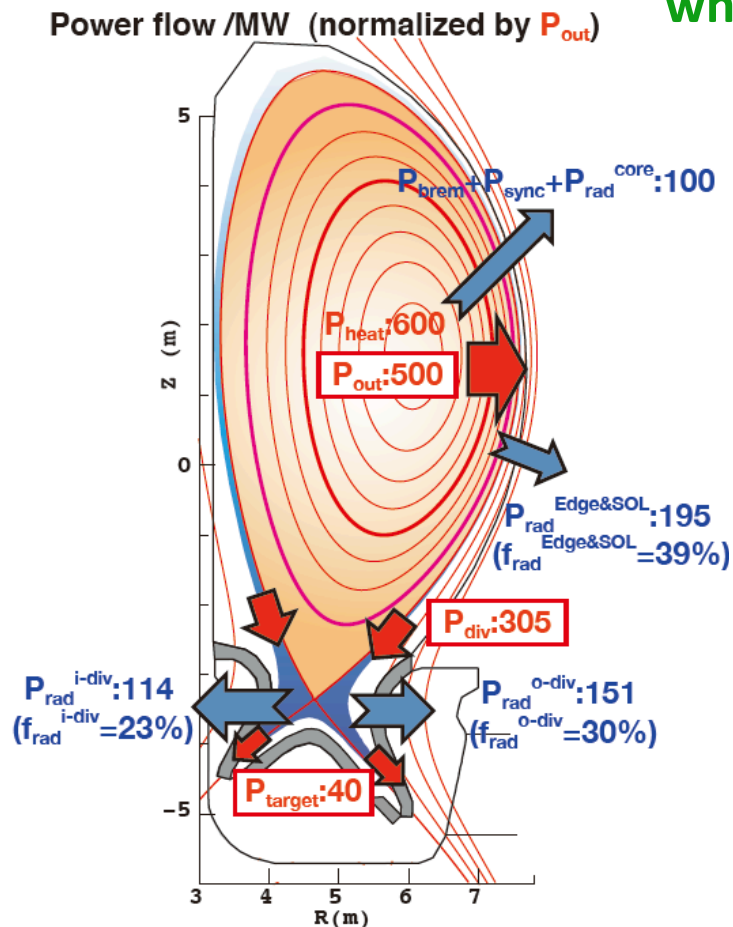
Full detachment in the outer divertor was obtained with increasing Ar puff rate both from midplane ($\Gamma_{\text{Ar}}^{\text{mid}}=0.35 \times 10^{21}$ Ar/s) and divertor ($\Gamma_{\text{Ar}}^{\text{div}}=0.7 \times 10^{21}$ Ar/s), where large Ar backflow ($\Gamma_{\text{Ar}}^{\text{dom}}(\text{in}) = 8.4 \times 10^{21}$ Ar/s and $\Gamma_{\text{Ar}}^{\text{dom}}(\text{out}) = 10.5 \times 10^{21}$ Ar/s) as well as Ar recycling flux in the divertor significantly affected the detachment.

- *Low T_e and $T_i < 2$ eV were seen over wide area both at inner and outer targets*
 \Rightarrow **Full detachment was obtained** (except for $T_e \sim 5$ eV, $T_i \sim 24$ eV at outer upper area).

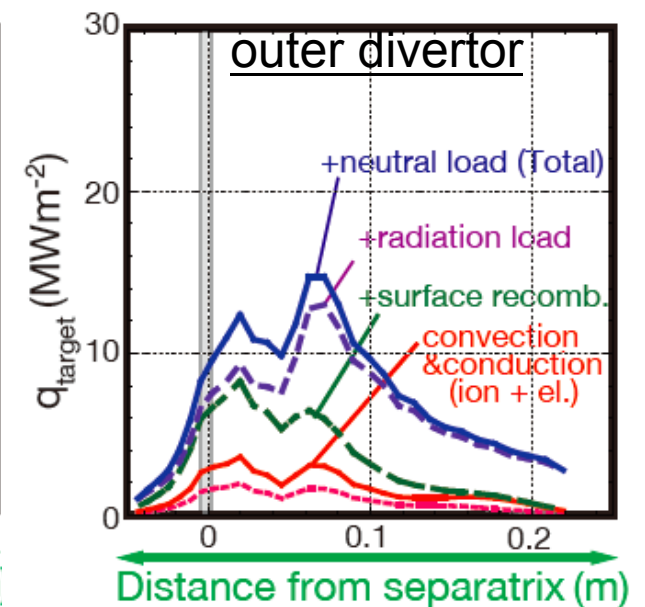
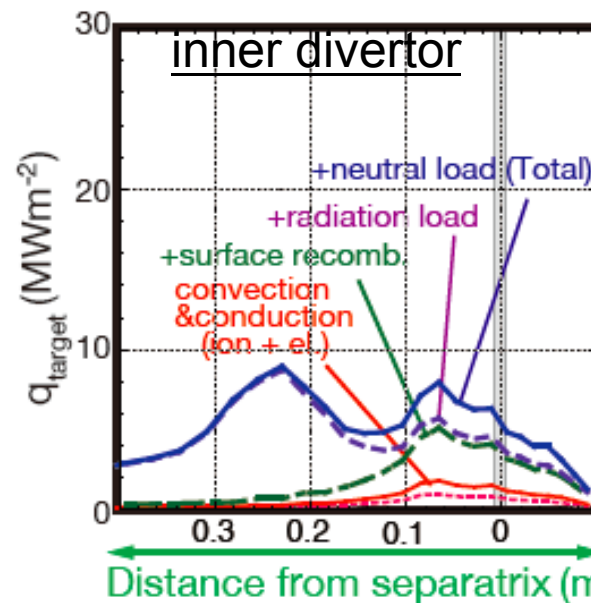


Radiation power load and neutral process in the detached divertor

- Full divertor detachment was produced when $P_{\text{rad}}^{\text{tot}}/P_{\text{out}}$ increased to $\sim 92\%$, where $P_{\text{rad}}^{\text{div}}/P_{\text{out}} = 53\%$ and $P_{\text{rad}}^{\text{Edge\&SOL}}/P_{\text{out}} = 39\%$ are distributed.
 - In the outer divertor, radiation source (Ar ions) was localized near the target \Rightarrow outer peak heat load (q_{target}) is $\sim 15\text{MWm}^{-2}$, while inner peak $q_{\text{target}} \sim 8\text{MWm}^{-2}$.
- Note: recombination of low-T ions contributes near the separatrix, while radiation load is small.**



Components of target heat load



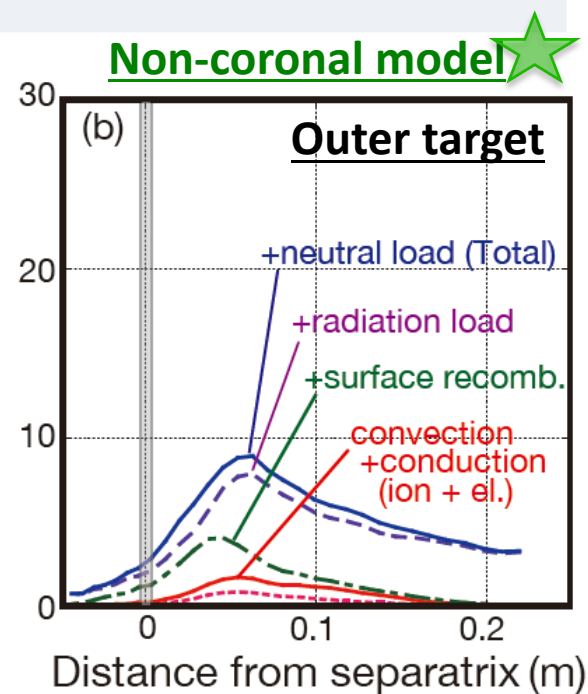
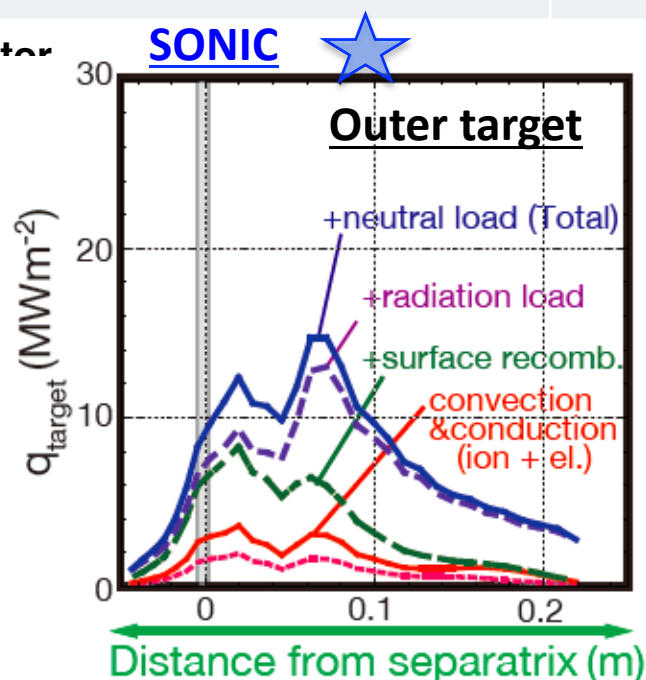
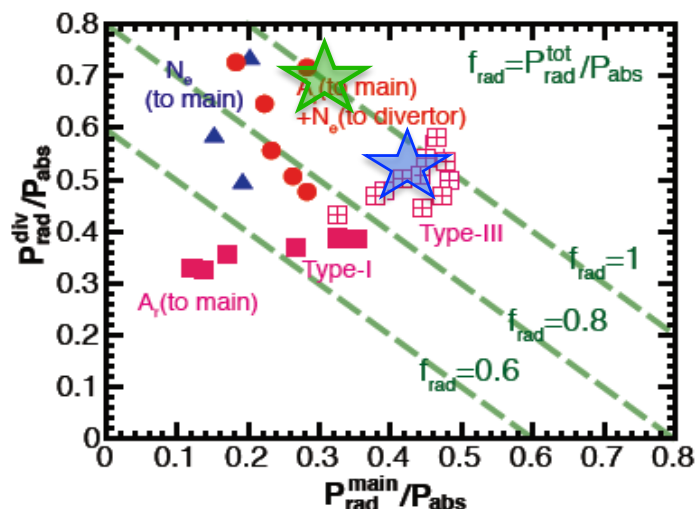
Radiation fraction and heat load components in full detached divertor

Radiation fraction at main/ divertor is comparable to experimental database.

Radiation power load is large, and components are similar to the previous result.

Radiation / heat loading	SONIC 	SOLDOR/NEUT2D 
Ar impurity transport	Self-consistent MC (assuming Ar-transport under dome)	Non-coronal model with constant $n_{Ar}/n_i [= f_{Ar}]$
$P_{rad}^{Edge\&SOL} (f_{rad}^{Edge\&SOL})$	195 MW (39%)	158 MW (31%) [$f_{Ar}=1\%$]
$P_{rad}^{i-div} (f_{rad}^{i-div})$	114 MW (23%)	97 MW (19%) [$f_{Ar}=1\%$]
$P_{rad}^{o-div} (f_{rad}^{o-div})$	151 MW (30%)	238 MW (48%) [$f_{Ar}=5\%$]
$P_{rad}^{tot} (f_{rad}^{tot})$	460 MW (92%)	493 MW (98%)
Peak q (trans/recom/rad)	3.2/ 3.3/ 6.3 MWm ⁻²	2.1/ 1.5/ 4.6 MWm ⁻²

Ex.1 Radiation fractions at main / divertor for Ar and/or Ne seeding in JT-60U



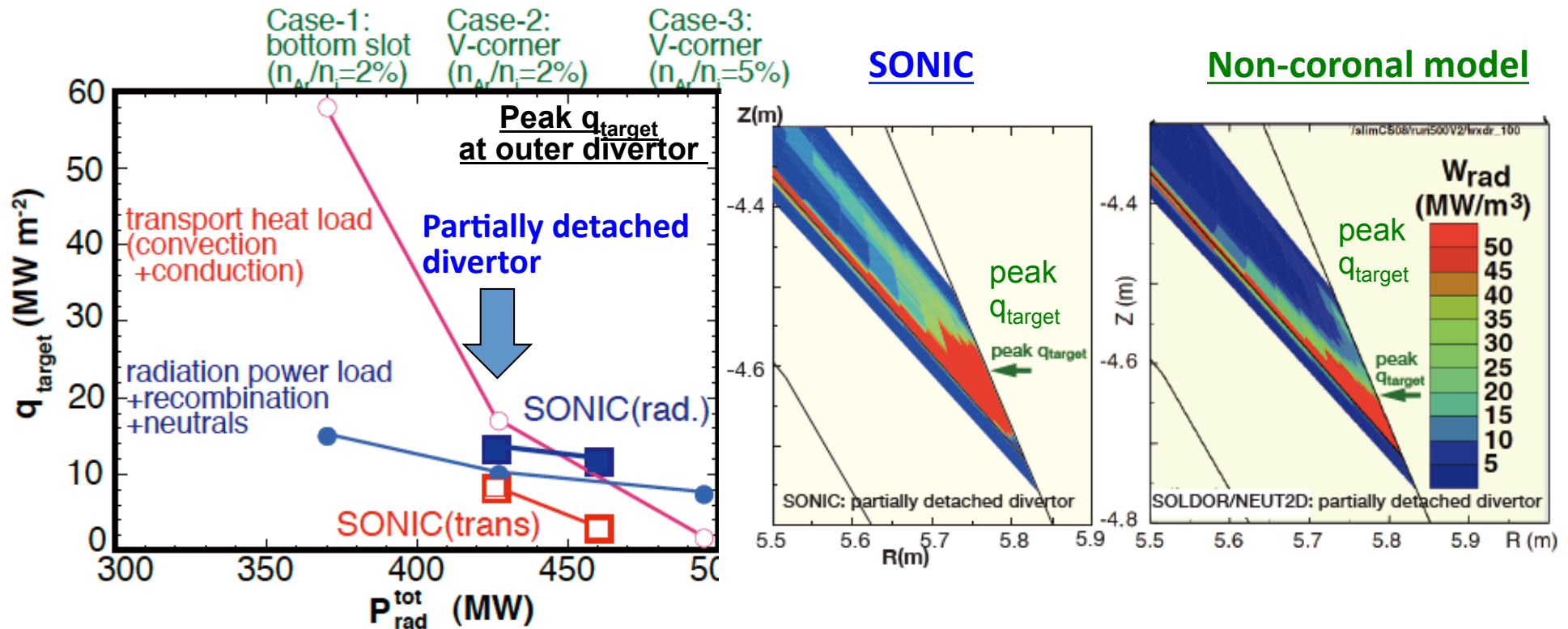
Radiation region more extends over the target in SONIC result \Rightarrow

Transport heat load is reduced, while radiation heat load is comparable

- For the similar $P_{\text{rad}}^{\text{tot}}$ ($\sim 425\text{MW}$) cases in partially detached divertor, where $P_{\text{rad}}^{\text{edge\&SOL}} = 165$ (SONIC)/ 160 (Case-2) and $P_{\text{rad}}^{\text{O-div}} = 156$ (SONIC)/162 MW (Case-2), peak heat load by plasma transport ($q_{\text{target}}^{\text{trans}} = 8 \text{ MW/m}^2$) for SONIC is smaller than Case-2 ($q_{\text{target}}^{\text{trans}} = 15 \text{ MW/m}^2$) since T_e^{div} at the peak q_{target} ($\sim 6 \text{ eV}$) is smaller than that for Case-2 ($\sim 13\text{eV}$).

For SONIC result, radiation area (A_r concentration) extends over the target

\Rightarrow Radiation power load ($q_{\text{target}}^{\text{rad}} = 14 \text{ MW/m}^2$) is slightly larger.

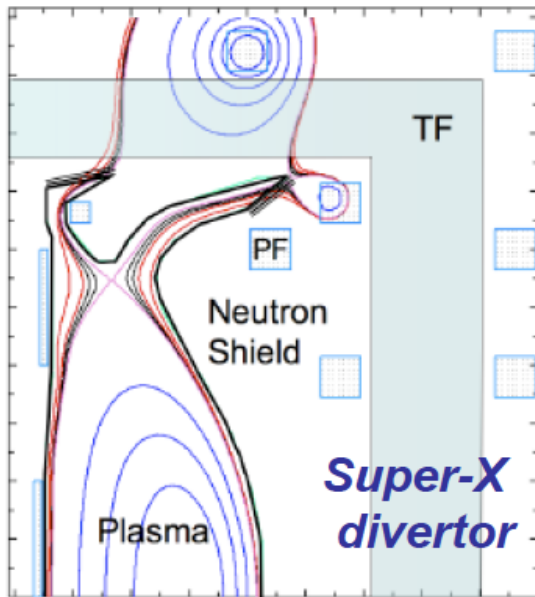


4. Extension of ITER divertor concept to DEMO divertor ?

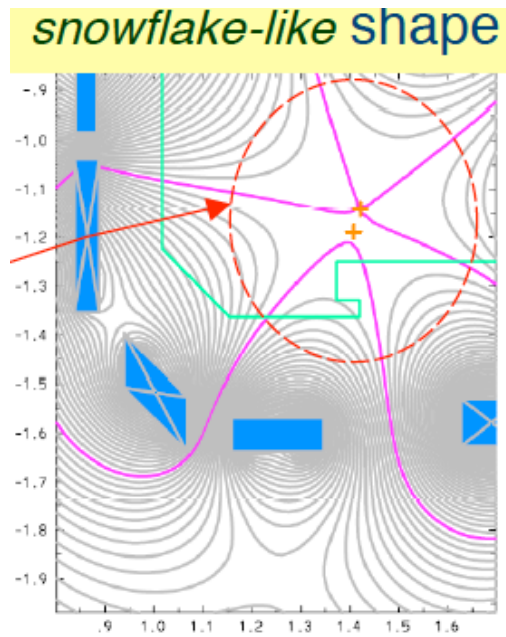
“Full detachment” is necessary for DEMO divertor, extending from ITER divertor
 ⇒ operation scenario of the divertor and main plasmas will be restricted by requirement of the high radiation loss and high edge density.

Design concept for DEMO divertor may be investigated from different viewpoints

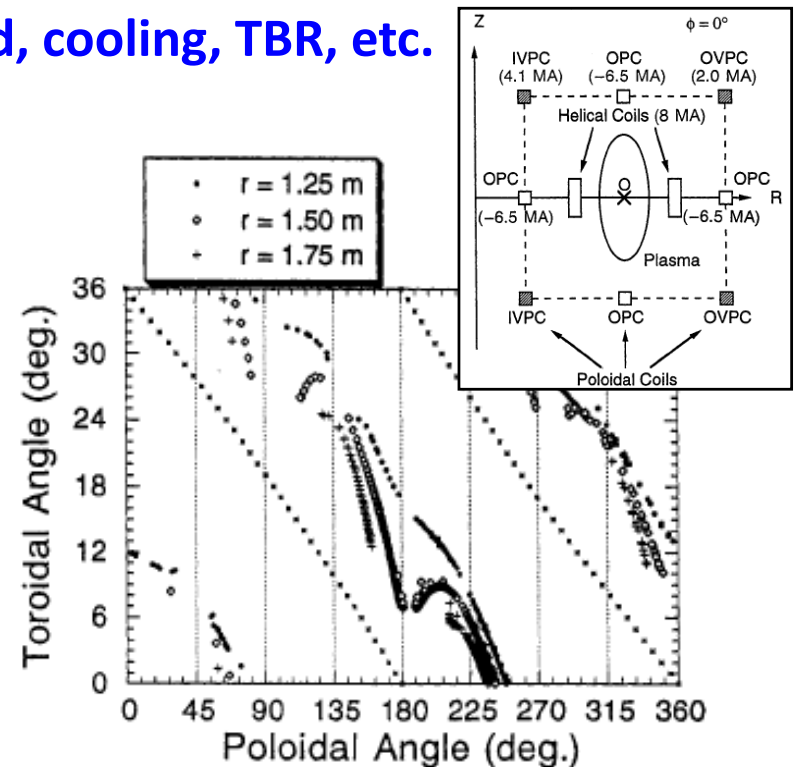
- (1) Super-X divertor ⇒ Divertor leg and target area are increased
 long field-line and extending area to reduce T_e^{div} and q_{target} .
 - (2) Snowflake-like divertor ⇒ Flux expansion and effective field-line length
 - (3) Helical field ⇒ Enhancing diffusion by magnetic perturbation
- ⇔ Coil design issues are remained: neutron shield, cooling, TBR, etc.



Kotschenreuther



Ryutov, Phys. Plas. 14 (2007) 064502



Iakase, et al, NUCL. FUSION 35 (1995) 123

5. Summary: Progress in simulation study for DEMO divertor

Huge power handling ($P_{\text{out}} = 500\text{MW}$) for SlimCS ($P_{\text{fusion}} \sim 3\text{GW}$) was investigated.

- SONIC with impurity MC has been developed for the Ar impurity seeding.

Conversion of divertor plasma became more stable by recent developments:

- (1) **“flux limiter” for ion conduction transport** : $q_i^{\text{conv}} = n_i k(T_i^{5/2}) \nabla T_i < 0.5 n_i v_{\text{th-i}} T_i$,
- (2) **distribution of Ar atoms and particle balance under the divertor (exhaust route)** were calculated in the similar condition (simulating a steady-state).

Self-consistent coupling of the fluid plasma, MC neutral and MC impurity (Ar) **“in steady-state”** was obtained *with comparable time scale (~50ms)*.

- Full detachment was obtained (*low* T_e^{div} and $T_i^{\text{div}} < 2$ eV were seen over wide area) when $P_{\text{rad}}^{\text{tot}}/P_{\text{out}}$ increased to **~92%** ($P_{\text{rad}}^{\text{div}}/P_{\text{out}} = 53\%$ and $P_{\text{rad}}^{\text{Edge\&SOL}}/P_{\text{out}} = 39\%$).

⇒ **Outer peak q_{target} was $\sim 15\text{MWm}^{-2}$ and inner peak $q_{\text{target}} \sim 8\text{MWm}^{-2}$, which were attributed mostly to radiation power and neutral flux** than plasma heat flux.

Radiation power load changed gradually for SONIC and non-coronal model.

SONIC showed that large radiation region extends to the outer flux surfaces over the outer target

⇒ **transport heat load was reduced efficiently over the wide area, compared to non-coronal model.**

Future plans for power exhaust simulation

Radiation power load is dominant, and control of the radiation power and distribution is important.

- **Radiation region/distribution would be control by**
 - (1) different impurity species such as Ne, Kr, Xe, etc. and puff locations,**
 - (2) geometry of target inclination and V-corner shape,**
 - (3) impurity transport (pinch/diffusion) in edge will be considered in core-edge boundary region (now $r/a > 0.95$ is treated).**
- **Magnetic expansion in the target and shear effect such as snow-flake will be investigated in different divertor coil configurations.**
- **Photon absorption by dense divertor plasma will affect distribution of the detachment plasma → including the atomic model for absorption.**

Estimation of computer time for steady-state distribution($t \sim 1s$)

JAEA parallel computer: effective speed 20GFlops

IFARC parallel computer: effective speed 100TFlops

$$100TFlops/20GFlops = 5000 \text{ times faster}$$

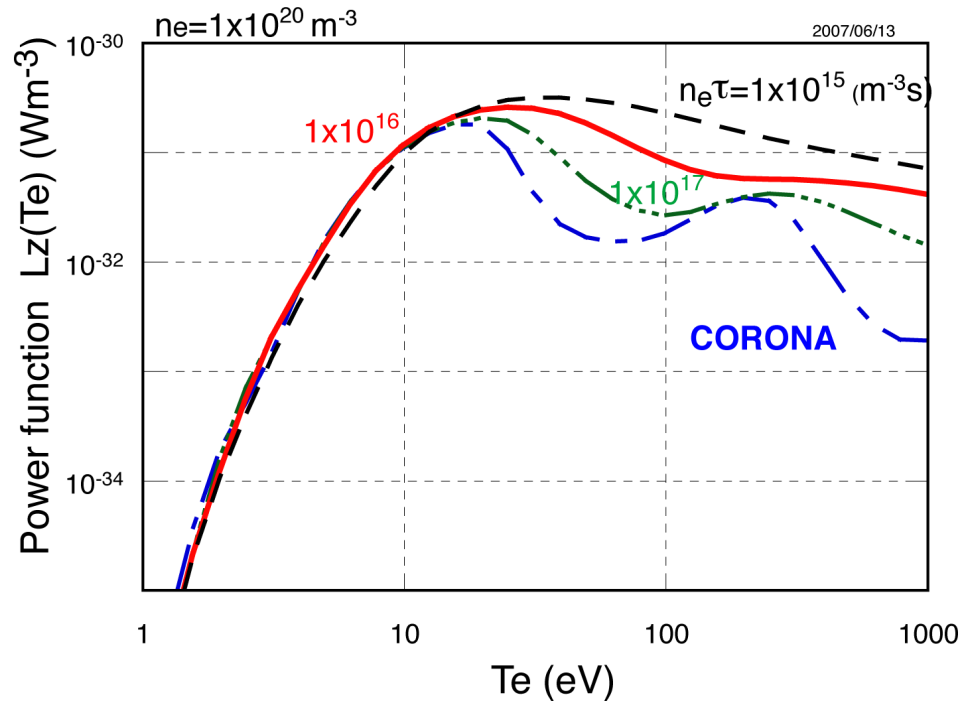
SONIC calculation: 3ms \sim 9 hours

$$1s/0.003s = 333 \text{ times more required}$$

Then, SONIC calculation in steady-state (1s) will need

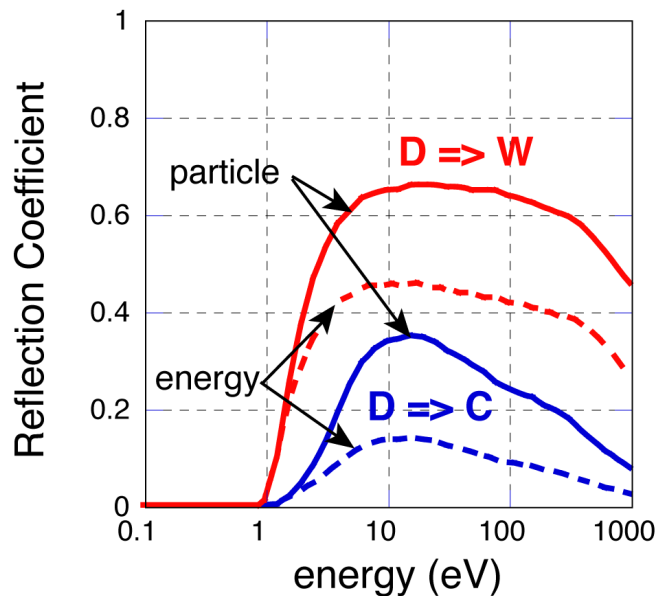
$$9 \text{ hrs} \times 333/5000 = 0.6 \text{ hr}$$

Impurity and neutral treatment



Impurity radiation: non-coronal model

- Ar fraction (n_{Ar}/n_i) is given.
- Radiation loss power is evaluated by $W_r = -n_e n_z L_z(T_e)$.
- Loss rate $L_z(T_e)$ is used on $n_e \tau_{\text{res}} = 1 \times 10^{16} \text{ s/m}^3$.



Neutral reflection: W target model

- Assumed W wall, which reflection coefficients of particle and energy are almost twice larger than that for carbon.